Heliyon 10 (2024) e35266

Contents lists available at ScienceDirect

Heliyon

journal homepage: www.cell.com/heliyon

Research article

Safety assessment of electrosurgical electrodes by using mini pig tissue

Xin Rui Zhang [a,b,1], Thuy-Tien Thi Trinh [b,c,d,1], Pham Ngoc Chien [b,c,d], Nguyen Ngan Giang [b,e], Shu Yi Zhou [a,b], Sun Young Nam [b,*], Chan Yeong Heo [a,b,c,d,e,**]

[a] Department of Plastic and Reconstructive Surgery, College of Medicine, Seoul National University, Seoul, Republic of Korea
[b] Department of Plastic and Reconstructive Surgery, Seoul National University Bundang Hospital, Seongnam, Republic of Korea
[c] Korean Institute of Nonclinical Study Center, Seongnam, Republic of Korea
[d] H&BIO Corporation/R&D Center, Seongnam, Republic of Korea
[e] Department of Medical Device Development, College of Medicine, Seoul National University, Seoul, Republic of Korea

A R T I C L E I N F O

Keywords:
Electrosurgery
Electrosurgical electrodes
Safety
Thermal tissue effect

A B S T R A C T

Electrosurgical electrodes are the main dissecting devices widely used for surgeries throughout the world. The present study aimed to evaluate the thermal injury and safety within animals' organs following a minimally invasive electrosurgery technique with electrosurgical electrode AE40-300 (LIPO) and AE20-80 (LIFT). To ensure the effective application of electrosurgery in a clinical environment, it is crucial to minimize heat-induced injury to nearby tissues. In this study, the skin, liver, kidney, and femoral muscle dissected from 9 minipigs were used in tissue thermal spread experiments. Thermal imaging area analysis, maximum temperature, and time to reach basal temperature were evaluated. Thermography results revealed that the surgical temperature was significantly lower in the minimally invasive electrosurgery with AE40-300 (LIPO) and AE20-80 (LIFT) compared to the predicate device. In addition, AE40-300 (LIPO) and AE20-80 (LIFT) created a relatively small thermal injury area and thermal diffusion. Our results indicated that the tested devices named AE40-300 (LIPO) and AE20-80 (LIFT) reduced excessive thermal injury and could be applied to clinical use safely.

1. Introduction

Electrosurgery is a medical technique that utilizes high-frequency electrical current to cut, coagulate, or remove tissue during surgical procedures. In the operating theater, it is a widely used method across various medical specialties due to its precision and effectiveness in controlling bleeding, dissecting tissue, and achieving surgical objectives by vaporization, desiccation, coagulation and fulguration.

* Corresponding author. Department of Plastic and Reconstructive Surgery, Seoul National University Bundang Hospital: 172 Dolmaro, Bundang-gu, Seongnamsi, 13620, Republic of Korea.

** Corresponding author. Department of Plastic and Reconstructive Surgery, College of Medicine, Seoul National University Address: 103 Daehak-ro, Jongno-gu, Seoul, 03080, Republic of Korea.

E-mail addresses: 99261@snubh.org (S.Y. Nam), lionheo@snu.ac.kr (C.Y. Heo).

[1] These authors contributed equally to this manuscript.

https://doi.org/10.1016/j.heliyon.2024.e35266
Received 16 January 2024; Received in revised form 24 July 2024; Accepted 25 July 2024
Available online 26 July 2024

The earliest example of using heat for treatment dates back as far as prehistoric times, describing a therapeutic tool named "cautery". It was heated and applied to the tissue to treat tumors. The application of conductive heat to tissues gained recognition in medicine as early as around the third century BC [1–5]. In the late 19th, Tesla's work in alternating current (AC) laid the foundation for understanding electrical properties that would later contribute to electrosurgery. In 1881, Morton discovered that alternating current with a frequency of 100 KHz could traverse through the human body without inducing neuro-muscular stimulation or causing electric shock [2,4,5]. In 1891, French physicist Alex d'Arsonval demonstrated that radio-frequency currents could heat living tissue without muscle or nerve stimulation, and he did note that the current directly influenced body temperature, oxygen absorption, and carbon dioxide elimination, increasing each as the current passed through the body [6]. Of note, the temperature was determined to increase proportionally to the square of the current density. In the early 20th century, Harvard biophysicist William Bovie produced a commercially available electrosurgical unit (ESU) that utilized high-frequency alternating current to cut and coagulate tissues effectively. Dr. Harvey Cushing popularized the utilization of Bovie's ESU (Electrosurgical Unit) through his performance of surgical procedures previously deemed unfeasible when he used it to remove an enlarging, vascular myeloma from the head of a 64-year-old patient [1,2,7–9].

While it is a commonly used technique in various surgical specialties due to its efficiency and precision, unintended thermal tissue effects were the most common complication associated with electrosurgery [5,10–12]. Uncontrolled or prolonged exposure to the electrical current can cause thermal burns to the tissue, both at the surgical site and surrounding areas. And overheating or improper use of electrosurgical devices can lead to unintended damage to surrounding healthy tissues, affecting their function or causing complications [11,13]. In addition, excessive thermal effects can hinder the normal healing process of tissues, leading to delayed wound healing or other healing complications [14–16].

Electrosurgical electrodes play a crucial role in the safety and efficacy of surgical procedures. First, the type of electrode and its surface area in contact with tissue influence how electrical energy is dispersed [2,17]. Different electrode designs are used for specific purposes such as precise cutting, coagulation, or fulguration. Proper selection of electrodes ensures the desired tissue effect, minimizing collateral damage to surrounding tissues [18–20]. Second, electrodes must efficiently dissipate heat to prevent excessive tissue damage. Improved electrode designs incorporate features to manage heat, reducing the risk of thermal injury to adjacent tissues. Third, electrodes can be made from various materials and may have specialized coatings to enhance their performance. Insulation materials prevent unintended energy dispersion and protect adjacent tissues from damage. Coatings can enhance conductivity and minimize tissue adhesion, reducing the risk of tissue sticking to the electrode [21–25]. Moreover, the size and shape of electrodes influence their precision and effectiveness. Smaller electrodes offer finer control for delicate procedures, while larger ones are suitable for broader tissue coverage. Proper sizing and shaping of electrodes contribute to the safety and efficacy of the surgical technique. Changes in the contact area of the active electrode can affect the current density, which will have a remarkable impact on safety and effectiveness [26–28].

A decrease in the size of the electrode is known to result in a higher current concentration, which means that if the contact area of the active electrode is reduced by a factor of 10, the current density would increase by a factor of 100 without any alteration in the power setting [2,4,29]. Hence, the size of the electrodes used during electro-surgical strongly effects the safety and effectiveness of the electro-surgical devices.

In this study, we aim to evaluate the safety, specifically the thermal tissue effects, of two examined electrosurgical electrodes: AE40-300 (LIPO) with the largest diameter electrode, and AE20-80 (LIFT) which is smallest diameter model.

We prepared three different electrosurgical electrodes, including two subject devices (AE40-300 (LIPO), AE20-80 (LIFT)), and one predicate device (Injectable RF Electrode K173582 (V-10-10-18-B-G2)). These electrodes vary in diameter and contact area resulting in different current density profiles.

The experiments involved the use of dissected skin, liver, kidney, and femoral muscle tissues from a total of nine mini pigs to conduct thermal tissue spread experiments. The safety and thermal effectiveness of each device were evaluated using several parameters, including thermal imaging area analysis, the maximum temperature reached, and the duration required to return to the basal temperature, which were assessed and analyzed in this study.

2. Materials and methods

2.1. Materials

The electrosurgical device (CWM-910T) and electrosurgical system electrodes (AE40-300(LIPO) and AE-20-80(LIFT)) were provided by Chungwoo Co., Ltd. (Seoul, Republic of Korea). Both electrodes were reusable electrosurgical electrodes.

Our study used the predicate device named CARVATI Temperature Controlled Radiofrequency (RF) System (Injectable RF Electrode K173582) (Mode: V-10-10-18-B-G2) which were provided by Chungwoo Co., Ltd. (Seoul, Republic of Korea).

2.2. Ethics statement

The Nonclinical Research Institute, CORESTEMCHEMON Inc. received approval from the AAALAC International for full accreditation in 2010. The present study was approved by the Institutional Animal Care and Use Committee (IACUC) of Nonclinical Research Institute, CORESTEMCHEMON Inc. (Serial No.: 2022-0688).

2.3. Animal preparation

Nine female-Designated Pathogen Free (DPF) Yucatan mini pigs (Medipig white hairless Yucatan) were purchased from Optipharm Co., Ltd. (Chungcheongbuk-do, Republic of Korea). The mini pig was selected since this species has been widely used in studies similar to this study and a large database exists for this species, so these data can be utilized in the interpretation and evaluation of the results of the study.

The animals were quarantined and acclimated for 6–13 days under the laboratory conditions. The animals were housed individually in stainless steel cages (W 108 × L 140 × H 120 cm) during the whole housing period. The animal breeding room was maintained at a temperature of 22 ± 3 °C and a relative humidity of 55 ± 15 %, ventilation of 10–20 air changes per hour, and a 12-hr light/12-hr dark cycle (from 08:00 to 20:00), 150–300 Lux of luminous intensity. The temperature and humidity of the animal room were measured every hour with a computer-based automatic sensor, and the environmental conditions such as ventilation frequency and luminous intensity were monitored regularly.

Each of the animals was provided 400 g of swine diet daily manufactured by Cargill Agri Purina, Inc (Gyeonggi-do, Republic of Korea). Disinfected water by ultraviolet sterilizer and ultrafiltration is given via an automatic water supplier, *ad libitum*. Examination of water was performed by an authorized Gyeonggi-do Institute of Health & Environment (Gyeonggi-do, Republic of Korea), and the quality satisfied the standards for the drinking water.

Animals were identified by tattoos on the auricle during the quarantine, acclimation and experimental period. Cages were identified by color-coded ID cards labelling the animal ID, and cage racks were given unique serial numbers. A study identification sheet was attached to the entrance of the animal room to identify the study. In addition, all animals were checked at least once a day for mortality and clinical signs. The body weight was measured at receipt and necropsy.

2.4. Necropsy and tissue collection

The mini pigs were euthanized at the facility following the standard operating guidelines outlined by the Korea Ministry of Food and Drug Safety (IACUC). The euthanasia process involved administering a mixed solution (1:1, v/v) of Zoletil (50 mg/mL) and Rompun, injected at a dose of 1 mL per 10 kg into the post-cervical muscle of the pig. Following anesthesia, the pig was humanely sacrificed by exsanguination from the axillary artery and vein. After confirming the absence of external abnormalities, tissues were carefully dissected from the carcass using non-thermal methods. The skin, liver, kidney, and femoral muscle tissues were isolated and trimmed to remove excess surrounding tissues.

Specifically, the skin was dissected, and the subcutaneous fat was removed. Immediately afterward, the tissues were placed in cold PBS and refrigerated to maintain their integrity for subsequent experiments.

All of the specimens were handled carefully to avoid drying out, becoming excessively hydrated, overheated, or frozen.

Detailed records of the necropsy results and photographic documentation were maintained and undertaken to document the necropsy procedure and findings.

2.5. Subject device treatment and thermal imaging analysis

The experiment began by retrieving stored tissues from the refrigerator and preparing them into appropriately sized pieces for the experiment. Subsequently, the subject device electrode, featuring two output modes (Retraction (Continuous) and eMulsify (Pulse)), intended for use with the electrosurgical device (CWM-910T), was prepared.

The tissue was then placed in a tray adjusted to the basal temperature, approximately 20 °C. Throughout the experiment, the tray was moistened with Phosphate-buffered saline (PBS) to prevent tissue dehydration [30].

Once the prepared tissue reached the basal temperature, a probe was inserted to a specific depth. Upon activating the thermal imaging camera in recording mode, electrical stimulation was applied at a predefined output (5W, 25W, or 50W). Stimulation ceased upon reaching the set temperature (35 °C, 53 °C, or 70 °C).

After stimulation, the recording with the thermal imaging camera terminated once the tissue returned to the basal temperature. Subsequently, the tissues utilized in the experiment were preserved in a 10 % neutral buffered formalin solution.

2.6. Predicate device treatment and thermal imaging analysis

All of the preserved tissues were prepared in the same conditions as the tissues used in the subject device's experiment.

The predicate device electrode in output modes (TERMI Tight) to be used in the electrosurgical device (ARVATI) was prepared and connected to the main device (ARVATI Temperature Controlled Radiofrequency (RF) System, ThermiGen, L.L.C., USA).

When the prepared tissue reached the basal temperature, the probe was inserted to a certain depth. After operating the thermal imaging camera in the recording mode, electrical stimulation was applied to a certain output (50W). The stimulation was stopped when the set temperature (35 °C, 53 °C, or 70 °C) was reached. After the stimulation, the thermal imaging camera recording was stopped when the tissue returned to the basal temperature. Finally, the tissues used in the experiment were stored in the 10 % neutral buffered formalin solution.

2.7. Histopathological analysis

The fixed tissues underwent histopathological analysis conducted by an external agency (Estend Bio, Republic of Korea). A paraffin block was prepared using a fully automatic tissue processor after trimming in the direction of a cutting line, which included the position where the device was inserted.

The thermal injury-induced necrosis around the wound area penetrated by the probe was monitored by histopathological quantitative analysis. Post-trimming, tissue slides were stained using hematoxylin and eosin (H&E), following which the region of interest (ROI) was observed and scrutinized using optical microscopy (BX61, Olympus, Japan). Image Pro software (Media Cybernetics, USA) was utilized as a quantitative analysis tool.

2.8. Statistical analysis

The data were statistically analyzed using the commercial program SPSS Statistics 12.0K for Medical Science. Data were analyzed by student's t-test comparison procedures for the comparison between the maximum output 50W results of the subject devices (AE40-300(LIPO) and AE-20-80(LIFT)) and the predicate device (INJECTABLE RF ELECTRODE(V-10-10-18-B-G2)). Welch's *t*-test was performed in case of non-equal variance. Differences with p-values below 0.05 were considered statistically significant.

3. Results

3.1. Animal observation

No abnormal signs were observed during the period of animal experiment.

The weight of the animals remained consistent throughout the entire experiment. At the received date, the mini pigs had an average

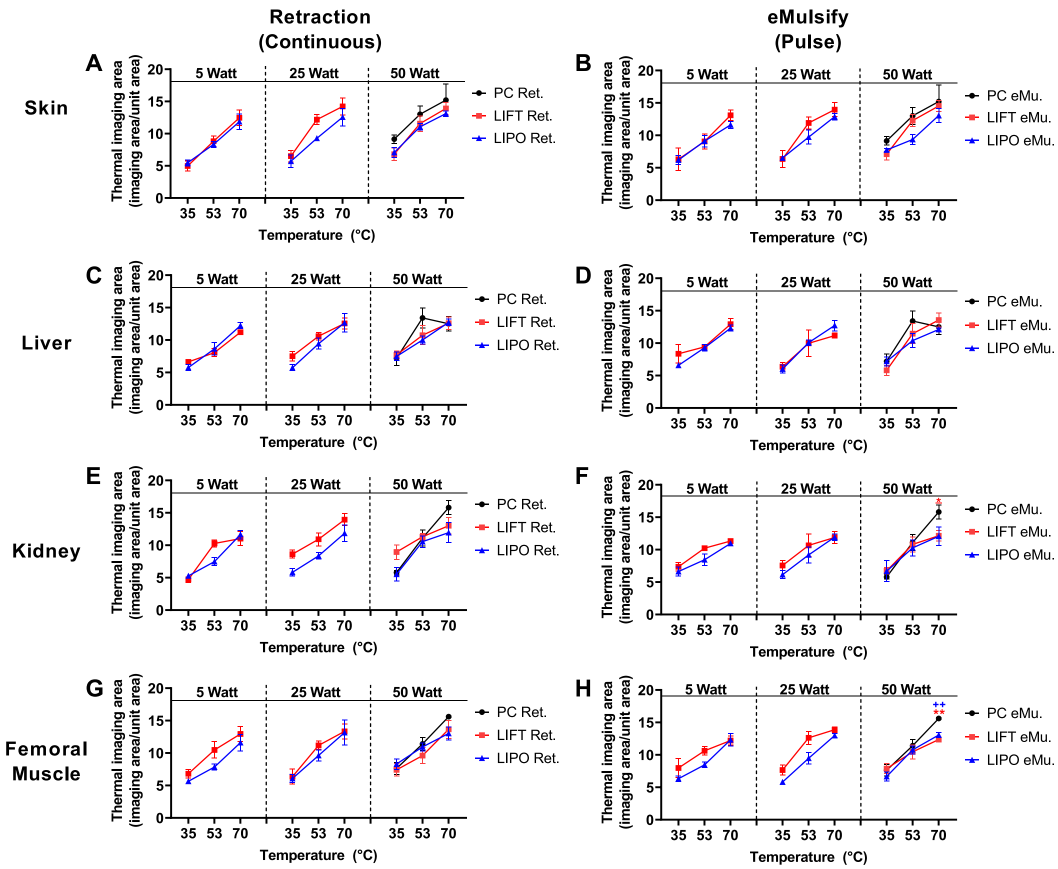

Fig. 1. Thermal imaging areas for each mode of skin (A–B), liver (C–D), kidney (E–F), femoral muscle (G–H) tissue. *Data were represented by mean ± S.E. The results were statistically analyzed by Student's t-test. Statistically difference between LIPO and Positive con. was presented as ++ with P < 0.01. Statistically difference between LIFT and Positive con. was presented as * (P < 0.05), ** (P < 0.01). Underline: Not equal variance (Welch's t-test). Ret.: Retraction (continuous) mode; eMu: eMulsify (pulse) mode. Subject devices: AE40-300 (LIPO) and AE20-80 (LIFT). Predicate device: Injectable RF Electrode (V-10-10-18-B-G2) (Positive con. (PC.)).*

body weight of 19.15 ± 0.63 kg, and their average body weight was not significantly changed on the necropsy day (after housing 9–13 days) which was measured as 19.21 ± 0.53 kg.

3.2. Thermography area analysis

The thermal image area was corrected by calculating a correction factor in consideration of the size of each device. Initially, the correction factor was determined by using a thermal image camera to measure the heating area of each device. Consequently, the values obtained were 0.399 cm^2 for AE40-300 (LIPO), 0.203 cm^2 for AE20-80 (LIFT), and 0.112 cm^2 for the predicate device, respectively. The measured values were calculated by dividing each area by its corresponding correction factor of the device.

In all operational modes of the subject devices, the thermal imaging areas of the skin tended to reduce at 35 °C compared to the predicate device. Notably, the subject device AE40-300 (LIPO) demonstrated a significant decrease at 53 °C compared to the predicate device (Fig. 1A–B).

Regarding the liver thermal imaging areas, in the retraction (continuous) mode of all subject devices, there was a tendency for the area to decrease at 53 °C in comparison to the predicate device. However, in the eMulsify (pulse) mode, the subject device AE40-300 (LIPO) showed a reduction in the area at 53 °C compared to the predicate device, while the AE20-80 (LIFT) exhibited a decrease at 35 °C compared to the predicate device (Fig. 1C–D).

In the case of kidney thermal imaging areas across all operational modes of the subject devices, there was a trend toward decreased area at 70 °C compared to the predicate device (Fig. 1E–F). Particularly in the eMulsify (pulse) mode, the AE20-80 (LIFT) device demonstrated a significant reduction in the area at 70 °C compared to the predicate device ($P < 0.05$) (Fig. 1F).

Regarding the femoral muscle thermal imaging areas, the subject device AE40-300 (LIPO) indicated a tendency to decrease in the

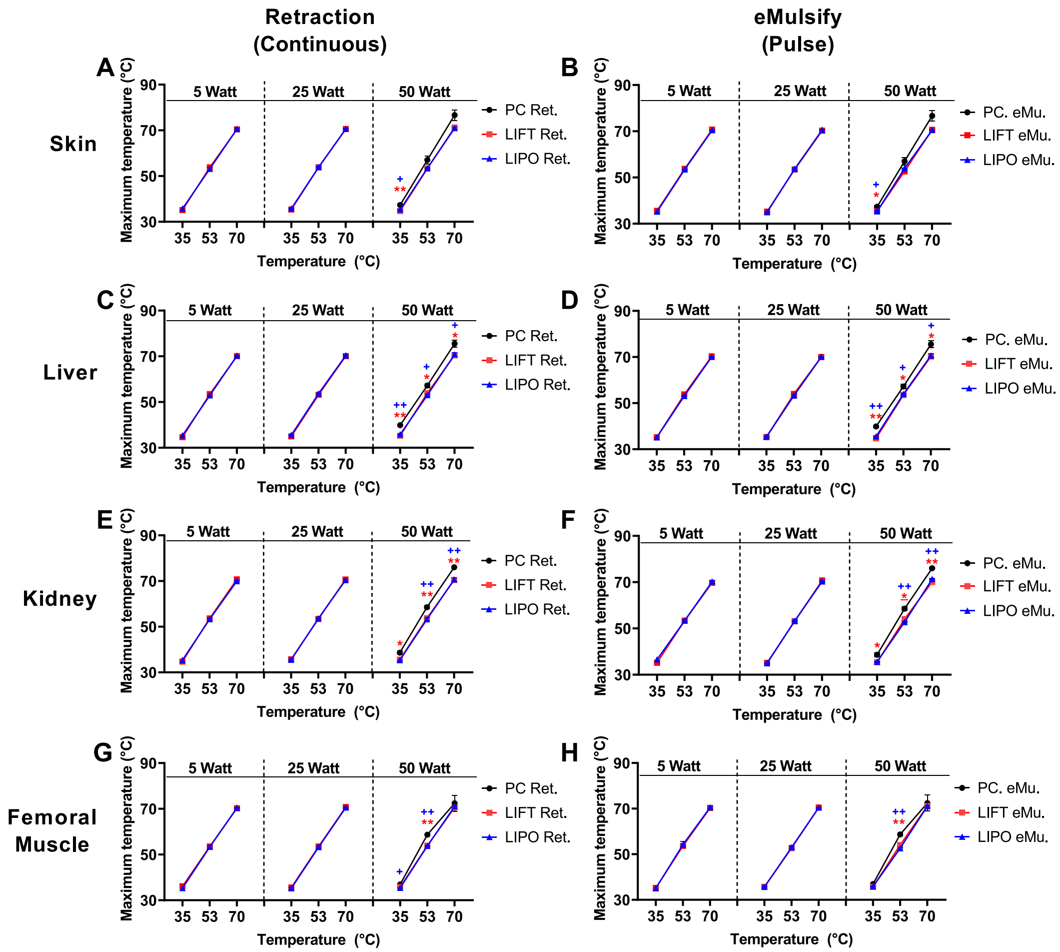

Fig. 2. The maximum temperatures for each mode of skin (A–B), live (C–D), kidney (E–F), femoral muscle (G–H) tissues.
Data were represented by mean ± S.E. The results were statistically analyzed by Student's t-test. Statistically difference between LIPO and Positive con. was presented as + with $P < 0.05$, and ++ with $P < 0.01$. Statistically difference between LIFT and Positive con. was presented as * ($P < 0.05$), ** ($P < 0.01$). Underline: Not equal variance (Welch's *t*-test). Ret.: Retraction (continuous) mode; eMu: eMulsify (pulse) mode. Subject devices: AE40-300 (LIPO) and AE20-80 (LIFT). Predicate device: Injectable RF Electrode (V-10-10-18-B-G2) (Positive con. (PC.)).

area at 70 °C compared to the predicate device in all operational modes (Fig. 1G–H). Specifically, in the eMulsify (pulse) mode, the AE40-300 (LIPO) showed a significant reduction in the area at 70 °C compared to the predicate device ($P < 0.01$). Moreover, in the retraction (continuous) mode, the subject device AE20-80 (LIFT) also demonstrated a trend toward decreased area at 53 °C compared to the predicate device. Additionally, in the eMulsify (pulse) mode, the AE20-80 (LIFT) exhibited a significant decrease in the area at 70 °C compared to the predicate device ($P < 0.01$) (Fig. 1H).

Notably, in all the tissues and the operational modes of subject devices, the LIFT device tends to reduce the thermal area compared to the LIPO device.

3.3. The maximum temperature

Across the skin, liver, and kidney tissues, all subject devices exhibited a tendency to reduce the maximum temperature at all specified temperature settings (35 °C, 53 °C, or 70 °C) in comparison to the predicate device. Especially within the skin tissue, the outcomes from all subject devices displayed a remarkable decrease in temperature at 35 °C (Fig. 2A–B). Concerning the liver tissue, all subject devices demonstrated a significant decrease in temperature across all designated settings (Fig. 2C–D). In kidney tissue, the AE40-300 (LIPO) device indicated a significant decrease in temperature at both 53 °C and 70 °C. Similarly, the subject device AE20-80 (LIFT) exhibited a significant temperature reduction at all set temperatures compared to the predicate device ($P < 0.05$ or $P < 0.01$) (Fig. 2E–F).

Regarding the femoral muscle tissue, all subject devices displayed a significant decrease in temperature at 53 °C compared to the predicate device ($P < 0.01$). Furthermore, the AE40-300 (LIPO) device showcased a significant temperature reduction at 35 °C compared to the predicate device ($P < 0.05$) (Fig. 2G–H).

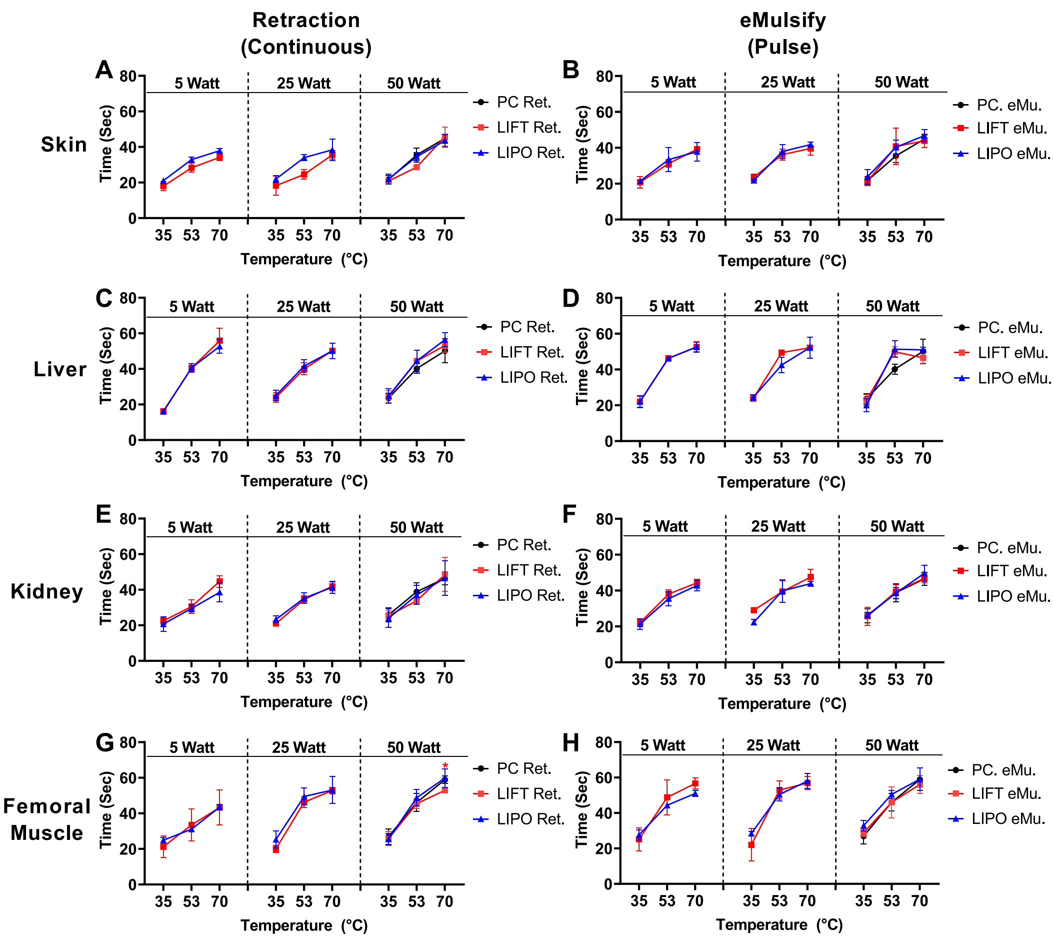

Fig. 3. Times reaching the basal temperature for each mode in skin (A–B), liver (C–D), Kidney (E–F), and femoral muscle (G–H) tissues. *Data were represented by mean ± S.E. The results were statistically analyzed by Student's t-test. Statistically difference between LIFT and Positive con. was presented as * ($P < 0.05$). Ret.: Retraction (continuous) mode; eMu: eMulsify (pulse) mode. Subject devices: AE40-300 (LIPO) and AE20-80 (LIFT). Predicate device: Injectable RF Electrode (V-10-10-18-B-G2) (Positive con. (PC.)).*

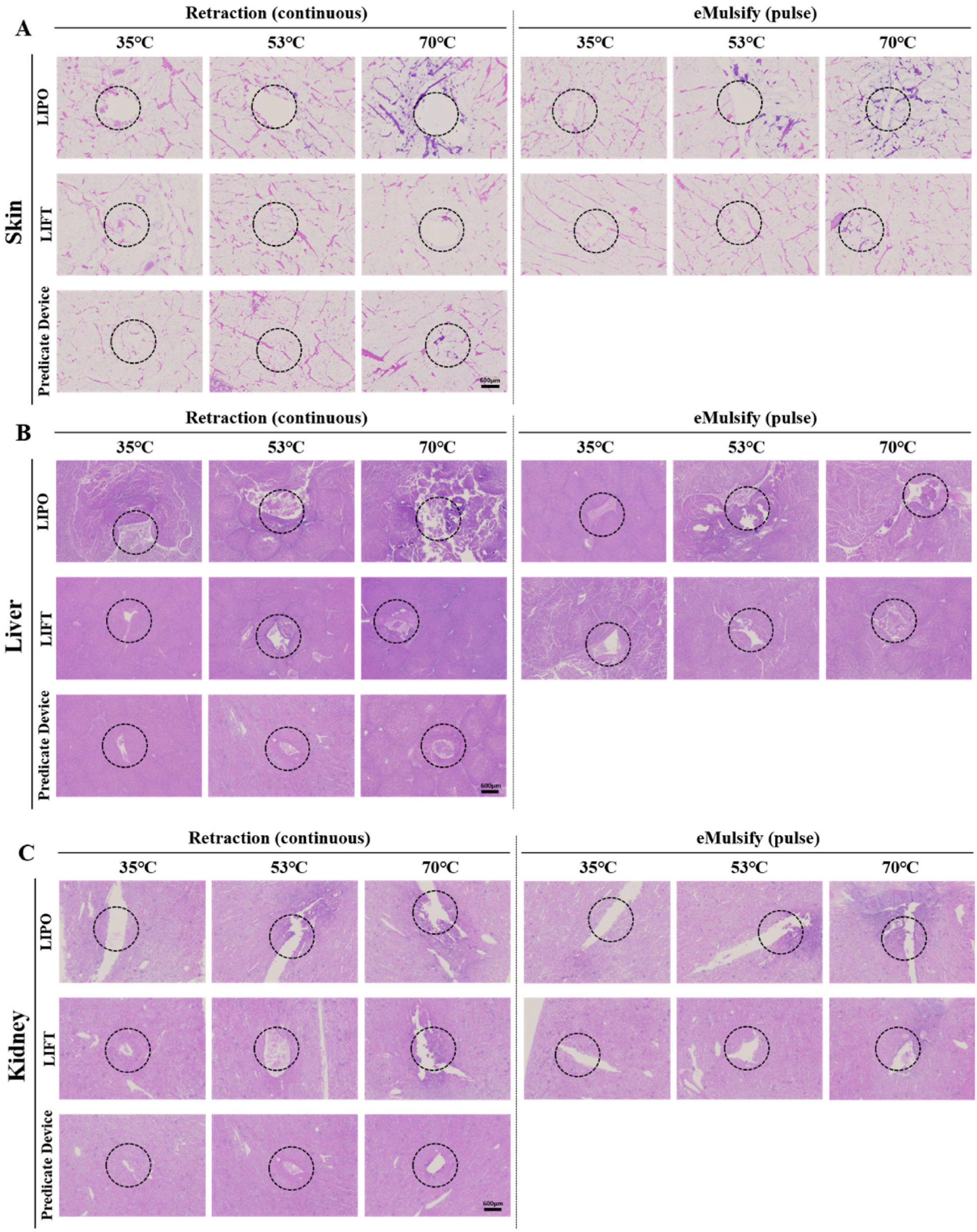

Fig. 4. Hematoxylin and eosin (H&E) staining of the thermal injury-induced necrosis areas for each mode of electrodes in skin (A), liver (B), kidney (C), and femoral muscle (D) tissues. *The dashed circle indicates the location of the surgical wound. Subject devices: AE40-300 (LIPO) and AE20-80 (LIFT). Predicate device: Injectable RF Electrode (V-10-10-18-B-G2). Scale bar: 600 μm.*

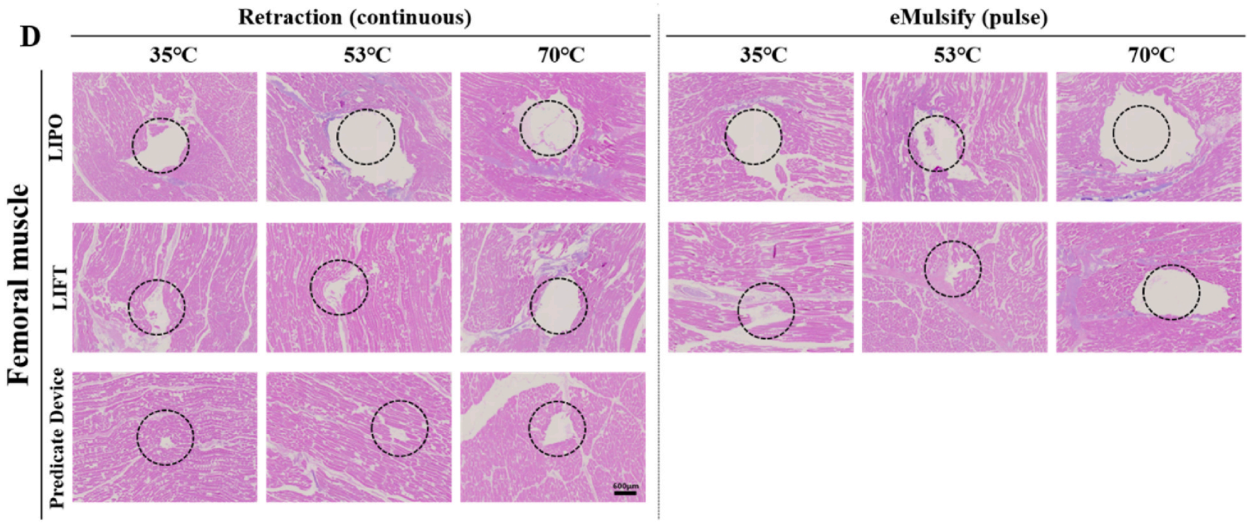

Fig. 4. (*continued*).

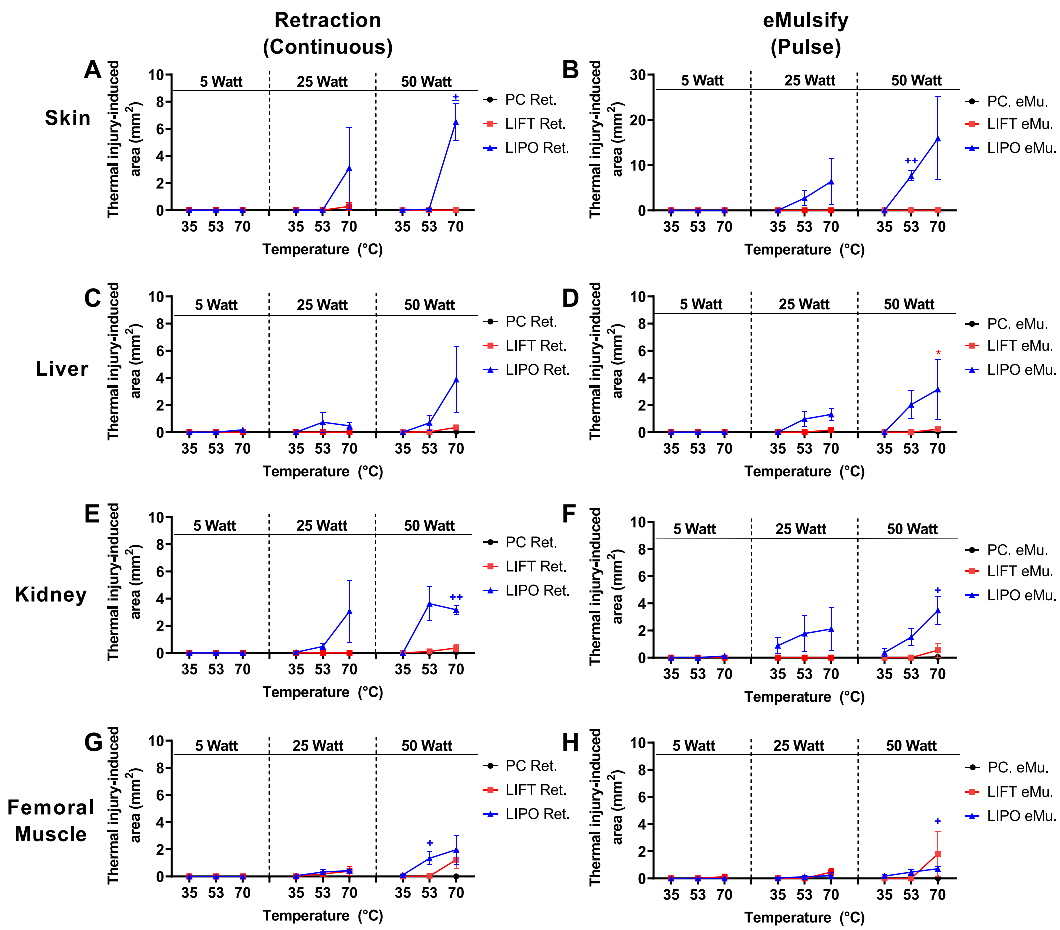

Fig. 5. Thermal injury-induced necrosis areas for each mode in skin (A–B), liver (C–D), Kidney (E–F), and femoral muscle (G–H) tissues. *Data were represented by mean ± S.E. The results were statistically analyzed by Student's t-test. Statistically difference between LIPO and Positive con. was presented as + with P < 0.05, and ++ with P < 0.01. Statistically difference between LIFT and Positive con. was presented as * (P < 0.05). Underline: Not equal variance (Welch's t-test). Ret.: etraction (continuous) mode; eMu: eMulsify (pulse) mode. Subject devices: AE40-300 (LIPO) and AE20-80 (LIFT). Predicate device: Injectable RF Electrode (V-10-10-18-B-G2) (Positive con. (PC.)).*

3.4. The duration required to return to the basal temperature

Based on the results of all tissues, the subject device AE40-300 (LIPO) exhibited no significant alteration in the time taken to return to the basal temperature compared to the predicate device (Fig. 3A–F, H). However, in the femoral muscle tissue, the results obtained from the retraction (continuous) mode of the subject device AE20-80 (LIFT) demonstrated a noteworthy decrease in the reduction time compared to the predicate device at 70 °C conditions ($P < 0.05$) (Fig. 3G).

3.5. Histopathological analysis

The histopathological analysis of the skin tissue revealed that the subject device AE40-300 (LIPO) displayed a noteworthy rise in thermal injury-induced necrosis area at 53 °C in eMulsify (pulse) mode and at 70 °C in retraction (continuous) mode compared to the predicate device, respectively ($P < 0.05$ or $P < 0.01$). It is worth noting that, across all modes, the subject device AE20-80 (LIFT) indicated a consistent tendency to decrease by more than 16 % in the area at 53 °C and 70 °C in comparison to the subject device AE40-300 (LIPO) (Figs. 4A and 5A–B).

In the liver tissue, the thermal injury-induced necrosis area under eMulsify (pulse) mode of the subject device AE20-80 (LIFT) was much bigger at 70 °C compared to the predicate device ($P < 0.05$) (Figs. 4B and 5C–D).

For kidney tissue, across all modes of subject devices AE40-300 (LIPO), there was a notable increase in the thermal injury-induced necrosis area at 70 °C compared to the predicate device ($P < 0.05$ or $P < 0.01$) (Figs. 4C and 5E–F).

In the femoral muscle tissue, the outcome from the retraction (continuous) mode of the subject device AE40-300 (LIPO) displayed a significant increase in the area at 53 °C compared to the predicate device ($P < 0.05$). Furthermore, the results from the eMulsify (pulse) mode of subject devices AE40-300 (LIPO) showed a significant increase in the area at 70 °C compared to the predicate device ($P < 0.05$) (Figs. 4D and Fig. 5G–H).

4. Discussion

Thermal tissue injury is a significant issue when performing electrosurgery in the operating room. As a result, there has been a significant emphasis among researchers on minimizing thermal tissue injury during electrosurgery [31–33].

To effectively avoid thermal injury when using an electrosurgical device, maintaining proper electrode size is necessary because using the smallest electrode size appropriate for the procedure to concentrate energy more effectively and minimize the area affected by heat. Additionally, managing the contact time of the electrode with tissue is another method to reduce injury as prolonged contact in one area can cause excessive buildup of thermal energy and lead to tissue damage. Moreover, the development of novel materials or coatings can indeed contribute to reducing thermal injury during electrosurgery. Materials with reduced adherence properties can prevent tissue from sticking to the electrosurgical instruments or electrodes [34,35].

Better insulation properties of materials can reduce the transmission of excessive heat to surrounding tissues and some coatings can dissipate heat more effectively, minimizing heat accumulation at the surgical site. For instance, in 1988, thermo-insulated plastic was developed and applied to the electrosurgery jaws, housing the metal conductor deep within the plastic. This innovation significantly decreased the extent of thermal injury. Surface treatment emerges as a viable method to alleviate thermal concentration and prevent overheating injuries [36].

In this study, both subject devices exhibited a tendency to decrease the thermal imaging area across all operation modes, signifying a potential for reduced thermal spread compared to the predicate device. Noteworthy, significant decline trends have been observed, in eMulsify mode, especially in the kidneys, and the hip muscle tissue at higher temperatures (70 °C). As for temperature, the subject devices consistently demonstrated lower maximum temperatures at various set temperatures (35 °C, 53 °C, or 70 °C) compared to the predicate device in different tissues. Specifically, the femoral muscle tissue revealed significant temperature reductions at 53 °C and tendencies to decrease at 70 °C with the subject devices. And all electrodes present similar performance in returning tissues to their baseline temperature after the procedures. Histopathological analyses indicated varying trends in thermal injury-induced necrosis areas across tissues. While both subject devices showcased tendencies to increase necrosis areas in kidney and femoral muscle tissues at higher temperatures (53 °C or 70 °C), the skin tissue analysis showed a tendency to decrease the area with the AE20-80 (LIFT) device. Additionally, the retraction (continuous) mode of the AE40-300 (LIPO) device displayed lower necrosis areas at specific temperatures compared to other tissues.

The study's findings collectively suggest that the subject devices generally exhibited reduced thermal impact on tissues. This is evidenced by decreased thermal imaging areas, lower maximum temperatures, and varied trends in thermal injury-induced necrosis areas across different tissues compared to the predicate device. The observed reductions in thermal spread and maximum temperatures with the subject devices imply a potential for minimized tissue damage and improved safety during electrosurgical procedures, particularly in sensitive tissues like the kidney and femoral muscles.

The present study investigated the thermal effects on different isolated tissues with no of both blood circulation, and body temperature, representing a specific limitation of our research. Tissue vasculature, implants, and pathological states of the body can considerably impact temperature distributions and heat transfer during surgery due to the thermal microeffect they create [37–39]. A thorough evaluation of these aspects is crucial to ensure accurate heat administration, avoiding thermal harm, and producing the ideal potential surgical results. Therefore, further investigations must be carried out to assess the influence of tissue temperature and blood flow on live animal surgical procedures.

Although the present study provides useful insights into the thermal impacts of the devices, future research might be improved by expanding the scope to include live animals and increasing the number of animals tested. Future research could delve deeper into specific modes of operation or examine long-term effects to better understand the devices' thermal impact comprehensively.

Including more factors or considering varied tissue types would enhance the overall knowledge of the thermal effects of the devices in different situations. Furthermore, ongoing research and validation in diverse clinical situations are crucial to guarantee the secure and efficient use of these devices in medical practice. These activities would increase our understanding and provide opportunities to improve and perfect the design and use of the devices, eventually improving patient outcomes and expanding the area of medical technology.

5. Conclusion

Overall, the subject device showed a tendency to decrease in maximum temperature at all set temperatures compared to the predicate device in the safety assessment of the subject device using mini pig tissues, indicating promising aspects of reducing the thermal impact associated with the subject devices, suggesting their potential for safer and more controlled electrosurgical procedures. However, continued research and validation in varied clinical scenarios are vital to fully comprehend their implications and ensure their safe and effective use in medical practice.

Funding

This work was supported by the Chungwoo Co., Ltd. (Seoul, Korea).

Data availability

All data to support the conclusions have been included in article and are clearly defined.

CRediT authorship contribution statement

Xin Rui Zhang: Writing – original draft, Visualization, Validation, Methodology, Investigation. **Thuy-Tien Thi Trinh:** Writing – review & editing, Writing – original draft, Visualization, Validation. **Pham Ngoc Chien:** Supervision, Investigation, Data curation, Conceptualization. **Nguyen Ngan Giang:** Visualization, Validation, Resources, Investigation. **Shu Yi Zhou:** Validation, Methodology, Investigation. **Sun Young Nam:** Writing – review & editing, Supervision, Funding acquisition, Conceptualization. **Chan Yeong Heo:** Writing – review & editing, Supervision, Resources, Project administration, Funding acquisition, Conceptualization.

Declaration of competing interest

The authors declare that they have no known competing financial interests or personal relationships that could have appeared to influence the work reported in this paper.

Acknowledgement

The authors would like to thank the Nonclinical Research Institute, CORESTEMCHEMON Inc. for experiment supports.

References

[1] J.L. O'Connor, D.A. Bloom, T. William, Bovie and electrosurgery, Surgery 119 (1996) 390–396, https://doi.org/10.1016/S0039-6060(96)80137-1.

[2] N.N. Massarweh, N. Cosgriff, D.P. Slakey, Electrosurgery: history, principles, and current and future uses, J. Am. Coll. Surg. 202 (2006) 520–530, https://doi.org/10.1016/j.jamcollsurg.2005.11.017.

[3] C.M. Jones, K.B. Pierre, I.B. Nicoud, S.C. Stain, W.V. Melvin, Electrosurgery, Curr. Surg. 63 (2006) 458–463, https://doi.org/10.1016/j.cursur.2006.06.017.

[4] M. El-Sayed, S. Mohamed, E. Saridogan, Safe use of electrosurgery in gynaecological laparoscopic surgery, Obstet. Gynaecol. 22 (2020) 9–20, https://doi.org/10.1111/tog.12620.

[5] M.M. El-Sayed, E. Saridogan, Principles and safe use of electrosurgery in minimally invasive surgery, Gynecol Pelvic Med 4 (2021), https://doi.org/10.21037/gpm-2020-pfd-10, 6–6.

[6] R.D. Tucker, C.R. Voyles, Laparoscopic electrosurgical complications and their prevention, AORN J. 62 (1995) 49–71, https://doi.org/10.1016/S0001-2092(06)63683-1.

[7] T.L. Smith, J.M. Smith, Radiofrequency electrosurgery, Oper Tech Otolaryngol Head Neck Surg. 11 (2000) 66–70, https://doi.org/10.1016/S1043-1810(00)80016-0.

[8] M.J. Russell, M. Gaetz, Intraoperative electrode burns, J. Clin. Monit. Comput. 18 (2003) 25–32, https://doi.org/10.1023/B:JOCM.0000025254.73456.db.

[9] C. Sutton, J. Abbott, History of power sources in endoscopic surgery, J. Minim. Invasive Gynecol. 20 (2013) 271–278, https://doi.org/10.1016/j.jmig.2013.03.001.

[10] R.C. Odell, Surgical complications specific to monopolar electrosurgical energy: engineering changes that have made electrosurgery safer, J. Minim. Invasive Gynecol. 20 (2013) 288–298, https://doi.org/10.1016/j.jmig.2013.01.015.

[11] G. Sankaranarayanan, R.R. Resapu, D.B. Jones, S. Schwaitzberg, S. De, Common uses and cited complications of energy in surgery, Surg. Endosc. 27 (2013) 3056–3072, https://doi.org/10.1007/s00464-013-2823-9.

[12] F. Brinkmann, R. Hüttner, P.J. Mehner, K. Henkel, G. Paschew, M. Herzog, N. Martens, A. Richter, S. Hinz, J. Groß, C. Schafmayer, J. Hampe, A. Hendricks, F. Schwandner, Temperature profile and residual heat of monopolar laparoscopic and endoscopic dissection instruments, Surg. Endosc. 36 (2022) 4507–4517, https://doi.org/10.1007/s00464-021-08804-4.

[13] M. Siddaiah-Subramanya, K.W. Tiang, M. Nyandowe, Complications, implications, and prevention of electrosurgical injuries: corner stone of diathermy use for junior surgical trainees, Surg. J. 3 (2017) e148–e153, https://doi.org/10.1055/s-0037-1606547.
[14] S. Guo, L.A. DiPietro, Factors affecting wound healing, J. Dent. Res. 89 (2010) 219–229, https://doi.org/10.1177/0022034509359125.
[15] X. Deng, M. Gould, M.A. Ali, A review of current advancements for wound healing: biomaterial applications and medical devices, J. Biomed. Mater. Res. B Appl. Biomater. 110 (2022) 2542–2573, https://doi.org/10.1002/jbm.b.35086.
[16] P. Schilrreff, U. Alexiev, Chronic inflammation in non-healing skin wounds and promising natural bioactive compounds treatment, Int. J. Mol. Sci. 23 (2022) 4928, https://doi.org/10.3390/ijms23094928.
[17] I. Alkatout, T. Schollmeyer, N.A. Hawaldar, N. Sharma, L. Mettler, Principles and safety measures of electrosurgery in laparoscopy, J. Soc. Laparoendosc. Surg. 16 (2012) 130–139, https://doi.org/10.4293/108680812X13291597716348.
[18] D.B. Jones, L.M. Brunt, L.S. Feldman, D.J. Mikami, T.N. Robinson, S.B. Jones, Safe energy use in the operating room, Curr. Probl. Surg. 52 (2015) 447–468, https://doi.org/10.1067/j.cpsurg.2015.08.004.
[19] H. Ferreira, C. Ferreira, Principle and use of electrosurgery in laparoscopy, in: A Manual of Minimally Invasive Gynecological Surgery, Jaypee Brothers Medical Publishers (P) Ltd, 2015, 69–69.
[20] D. Hema, J. Prasanna, Radiosurgery in periodontics: have we forgotten it? J. Indian Soc. Periodontol. 25 (2021) 6, https://doi.org/10.4103/jisp.jisp_48_20.
[21] C. Wu, F. Zhang, X. Xiao, J. Chen, J. Sun, D. Gandla, Y. Ein-Eli, D.Q. Tan, Enhanced electrochemical performance of supercapacitors via atomic layer deposition of ZnO on the activated carbon electrode material, Molecules 26 (2021) 4188, https://doi.org/10.3390/molecules26144188.
[22] P. Selinis, F. Farmakis, Review—a review on the anode and cathode materials for lithium-ion batteries with improved subzero temperature performance, J. Electrochem. Soc. 169 (2022) 010526, https://doi.org/10.1149/1945-7111/ac49cc.
[23] Z.C. Huertas, D. Settipani, C. Flox, J.R. Morante, T. Kallio, J.J. Biendicho, High performance silicon electrode enabled by titanicone coating, Sci. Rep. 12 (2022) 137, https://doi.org/10.1038/s41598-021-04105-x.
[24] M. Ryu, Y.-K. Hong, S.-Y. Lee, J.H. Park, Ultrahigh loading dry-process for solvent-free lithium-ion battery electrode fabrication, Nat. Commun. 14 (2023) 1316, https://doi.org/10.1038/s41467-023-37009-7.
[25] C.M. Vidhya, Y. Maithani, J.P. Singh, Recent advances and challenges in textile electrodes for wearable biopotential signal monitoring: a comprehensive review, Biosensors 13 (2023) 679, https://doi.org/10.3390/bios13070679.
[26] F. Hao, P.P. Mukherjee, Mesoscale analysis of the electrolyte-electrode interface in all-solid-state Li-ion batteries, J. Electrochem. Soc. 165 (2018) A1857–A1864, https://doi.org/10.1149/2.1251809jes.
[27] M.R. Domalanta, J.N. Bamba, D.D. Matienzo, J.A. del Rosario-Paraggua, J. Ocon, Pathways towards achieving high current density water electrolysis: from material perspective to system configuration, ChemSusChem 16 (2023), https://doi.org/10.1002/cssc.202300310.
[28] A. Indahlastari, A.L. Dunn, S. Pedersen, J.N. Kraft, S. Someya, A. Albizu, A.J. Woods, Impact of electrode selection on modeling tDCS in the aging brain, Front. Hum. Neurosci. 17 (2023), https://doi.org/10.3389/fnhum.2023.1274114.
[29] M.-P. Wu, C.-S. Ou, S.-L. Chen, E.Y.T. Yen, R. Rowbotham, Complications and recommended practices for electrosurgery in laparoscopy, Am. J. Surg. 179 (2000) 67–73, https://doi.org/10.1016/S0002-9610(99)00267-6.
[30] E.R. Cosman, J.R. Dolensky, R.A. Hoffman, Factors that affect radiofrequency heat lesion size, Pain Med. 15 (2014) 2020–2036, https://doi.org/10.1111/pme.12566.
[31] T.C. Wright, S. Gagnon, R.M. Richart, A. Ferenczy, Treatment of cervical intraepithelial neoplasia using the loop electrosurgical excision procedure, Obstet. Gynecol. 79 (1992) 173–178.
[32] R.L. Burns, A. Carruthers, J.A. Langtry, M.J. Trotter, Electrosurgical skin resurfacing: a new bipolar instrument, Dermatol. Surg. 25 (1999) 582–586, https://doi.org/10.1046/j.1524-4725.1999.98239.x.
[33] T.P. Moffitt, D.A. Baker, S.J. Kirkpatrick, S.A. Prahl, Mechanical properties of coagulated albumin and failure mechanisms of liver repaired with the use of an argon-beam coagulator with albumin, J. Biomed. Mater. Res. 63 (2002) 722–728, https://doi.org/10.1002/jbm.10389.
[34] K.-L. Ou, J.-S. Chu, H. Hosseinkhani, J.-F. Chiou, C.-H. Yu, Biomedical nanostructured coating for minimally invasive surgery devices applications: characterization, cell cytotoxicity evaluation and an animal study in rat, Surg. Endosc. 28 (2014) 2174–2188, https://doi.org/10.1007/s00464-014-3450-9.
[35] W.-T. Hsiao, L.-H. Lin, H.-J. Chiang, K.-L. Ou, H.-Y. Cheng, Biomedical electrosurgery devices containing nanostructure for minimally invasive surgery: reduction of thermal injury and acceleration of wound healing for liver cancer, J. Mater. Sci. Mater. Med. 26 (2015) 77, https://doi.org/10.1007/s10856-015-5416-4.
[36] W. Habermann, W. Müller, Tissue penetration of bipolar electrosurgical currents: joule overheating beyond the surface layer, Head Neck 35 (2013) 535–540, https://doi.org/10.1002/hed.22986.
[37] J. Shi, Z. Chen, M. Shi, Simulation of heat transfer of biological tissue during cryosurgery based on vascular trees, Appl. Therm. Eng. 29 (2009) 1792–1798, https://doi.org/10.1016/j.applthermaleng.2008.08.014.
[38] T.-C. Shih, H.-S. Kou, W.-L. Lin, Effect of effective tissue conductivity on thermal dose distributions of living tissue with directional blood flow during thermal therapy, Int. Commun. Heat Mass Tran. 29 (2002) 115–126, https://doi.org/10.1016/S0735-1933(01)00330-X.
[39] M. Maklad, A. Emam, Importance of postoperative use of external warming devices in flap reconstructive surgery, J Hand Microsurg 14 (2022) 271–275, https://doi.org/10.1055/s-0041-1727296.